Proceedings of the 32nd ISR (International Symposium on Robotics), 19-21 April 2001

Design of Artificial Finger Skin Having Ridges and Distributed Tactile Sensors

Daisuke Yamada*, Yoji Yamada** and Takashi Maeno*
*Department of Mechanical Engineering
Keio University
3-14-1 Hiyoshi, Kohoku-ku, Yokohama 223-8522 JAPAN
E-mail : ue06952@educ.cc.keio.ac.jp, maeno@mech.keio.ac.jp
**Toyota Technological Institute
2-12-1 Hisakata, Tempaku-ku, Nagoya 468-8511 JAPAN
E-mail : yamada@toyota-ti.ac.jp

Abstract

An artificial elastic finger for grasping an object, which we call an "artificial finger skin" is designed. Characteristics of the artificial finger skin are as follows: First, it has ridges at the surface and tactile sensors distributed underneath the ridges same as finger of human. Second, it has a curved surface in broad perspective. Third, it is made of an elastic silicone rubber so as to transform elastic deformation to the sensors. A Finite Element (FE) model of the artificial finger skin is made to conduct a dynamic contact analysis using a FE method in order to design the artificial finger skin in detail. As a result, it is confirmed that the designed artificial finger skin can detect partial incipient slippage of the ridge that occurs at the edge of the contact surface even when the weight and friction condition between the artificial finger skin and grasping object are changed.

1. Introduction

Human fingers allow an object to be lifted by an adequate grasping force without slippage, even when the weight and friction coefficient between the fingers and object are unknown. However, the mechanisms are not clearly understood. Johansson *et al.* [1][2] showed that the partial incipient slippage between the fingers and an object is important for grasping the objects with the fingers. However, relationship among contact condition, deformation of the skin and response of mechanoreceptors are not clarified.

In the field of robotics, a use of a robot hand to grip and lift an object is one of the most important problems. Several methods for grasping objects have been presented. One method is to pay attention to the detection of partial incipient slippage between the finger and object. This method is thought to be similar to what humans do. The partial incipient slippage refers to the contact condition between the robot fingers and grasping object in which a part of contact area slips while the other part sticks. This method was proposed first by Cutkosky *et al.* [3][4]. They detect the partial incipient slippage by sensing micro vibrations which are caused by an expansion of the slip regions within the contact area when a tangential force increases. The micro vibrations are detected by an accelerometers distributed near the contact area. However, this method is not adequate for precise positioning because the object moves slightly to the lifting direction due to the entire slippage. This method cannot be used as well when environmental vibrations or vibrations generated during multifinger manipulation occur. De Rossi *et al.* [5] made a device covered with silicone rubber and having distributed PVDF films as tactile sensors underneath the silicone rubber. The distributed tactile sensors can selectively be sensitive to shear and normal stress components. A neural network, whose inputs are outputs from the tactile sensors, provides a global sliding coefficient as an output. The partial incipient slippage between the device and objects are investigated. However, accuracy for detecting the global sliding slippage is not high enough, because the location of partial incipient slippage was not considered. Maeno *et al.* [6]-[8] showed that the shear strain distribution pattern inside an elastic finger indicates the stick/slip distribution at the finger surface during the precision grip. They also proposed a sensor capable of detecting the strain distribution inside the elastic finger having curved surface. The strain distribution is measured by strain gages embedded in the elastic finger. They showed a method for controlling the grasping force by use of proposed elastic robot finger as well. However, an object should be lifted by a certain speed. If the weight of object is changed while lifting the object, the object cannot be kept on grasping. Other methods in which the slippage is detected have been also presented. Yamada *et al.* [9] showed a slip sensor that has elastic ridges at the surface and is capable of isolating a stick-slip vibration due to an entire slippage between the sensor and grasping object. The sensor can detect the entire slippage and control the grasping force quickly and correctly to avoid dropping an object. However, the method is not adequate because the position of the object slightly changes due to the entire slippage.

In this study, an elastic finger skin that has a unique geometry imitating a configuration of ridges and FA I receptors (Meissner's corpuscles) of finger of human is

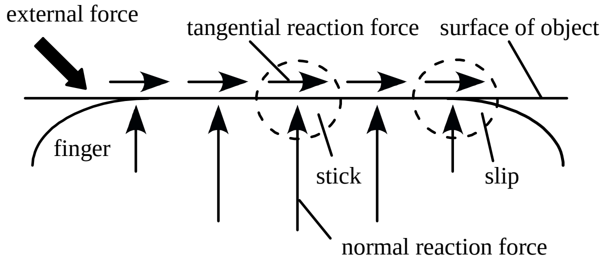

Fig. 1 Distribution of reaction force

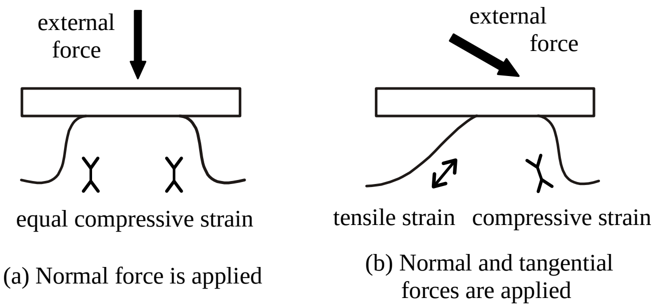

Fig. 2 Distribution of strain inside the ridge

proposed, which we call an "artificial finger skin". It can detect the partial incipient slippage of the ridges. It is designed by combining the method proposed by Maeno *et al*. [8] and Yamada *et al*. [9]. A design of the artificial finger skin is briefly described in chapter 2. Model and result of finite element (FE) analyses for validating the characteristics of designed artificial finger skin are shown in chapter 3. The conclusions of this study are described in chapter 4.

2. Design of artificial finger skin

2.1 What to mimic finger of human

Human can grasp an object by voluntary lifting speed of finger, even when the weight and friction coefficient between the finger and object are unknown. The artificial finger skin can be designed by imitating the characteristics of finger of human. The characteristics we paid attention to are as follows: First, the finger of human consists of flexible materials. The finger transforms contact information to the tactile receptors through an elastic deformation of tissues. Second, the finger of human has a curved surface in broad perspective. Third, epidermal ridges are distributed at the surface of finger. A pair of FA I receptors is located at the tip of dermis papilla underneath one epidermal ridge.

A partial incipient slippage easily occurs at the edge of the contact area between the fingers and object because the finger has curved surface. Figure 1 shows the reaction force distribution at the contact area. Normal reaction force at the center of contact area is larger than that at the edge of the contact area. However, tangential reaction force is almost equal throughout the contact area. The center of the contact area generally "sticks". However, the edge of the contact area easily changes its condition from "stick" to "slip" when the tangential force increases. Because of this, the partial incipient slippage occurs at the edge of the contact area.

When the partial incipient slippage occurs, elastic deformations are suddenly reduced at the ridges located at the edge of the contact area because the constraint due to the "stick" condition is released. The speed of movement of the ridge is constant which depend on the natural frequency of the ridge, even when the friction coefficient between the finger and object and the applied force changes.

A pair of FA I receptors are located near the border between the epidermis and dermis underneath the epidermal ridge. A stress concentration occurs at the location of FA I receptors. A strain distribution inside the ridges is closely related to the deformation of ridges as shown in Fig. 2. Only when the normal force is applied to the ridge as shown in Fig. 2 (a), the strain at the location of the pair of FA I receptors is symmetry. However, the strain at the pair of FA I receptors differs each other when both the normal and tangential forces are applied to the ridge as shown in Fig. 2 (b). If the strains at the pair of FA I receptors are subtracted, the value is zero when only the normal force is applied as shown in Fig. 2 (a). However, the subtracted value is not zero when the normal and tangential forces are applied as shown in Fig. 2 (b). Now, we can conclude that the deformation of the ridge in tangential direction can be detected by subtracting the strains at the two points underneath the ridge. Particularly, when the partial incipient slippage occurs, a velocity of the subtracted value decreases largely and an acceleration of the subtracted value becomes negative impulse at that time. It is expected that the partial incipient slippage can be detected by use of above-mentioned velocity and acceleration for controlling the grasping force, even when the weight and friction coefficient of the object and the applied force are unknown.

2.2 Detailed design

The artificial finger skin is designed in detail considering the above-mentioned characteristics of human finger.

First, a shape of ridges is decided. A relationship between the height of ridge and strain distribution inside the ridge is analyzed using FE analysis. Three types of FE models of one ridge are made. The height of ridge in each model is one-second, one-fifth and one-tenth of the width of the ridge, respectively. The shape of the ridge consists of a combination of several arcs. Friction coefficient is 1.0 in the analysis. Then, a flat object is set to be in contact with each model from the top. Figure 3 shows a distribution of strain inside the ridge. Too strong stress concentration occurs at the surface of the ridge in the model having high ridge as shown in Fig. 3 (a). Therefore, a large strain exists at the surface of the ridge. A durability of the ridge seems to be low. The strain is distributed near the surface of the ridge, and it is not transferred inside the ridge in the model having low ridge, even when the tangential force is applied as shown is Fig. 3 (c). Therefore, the subtracted value of

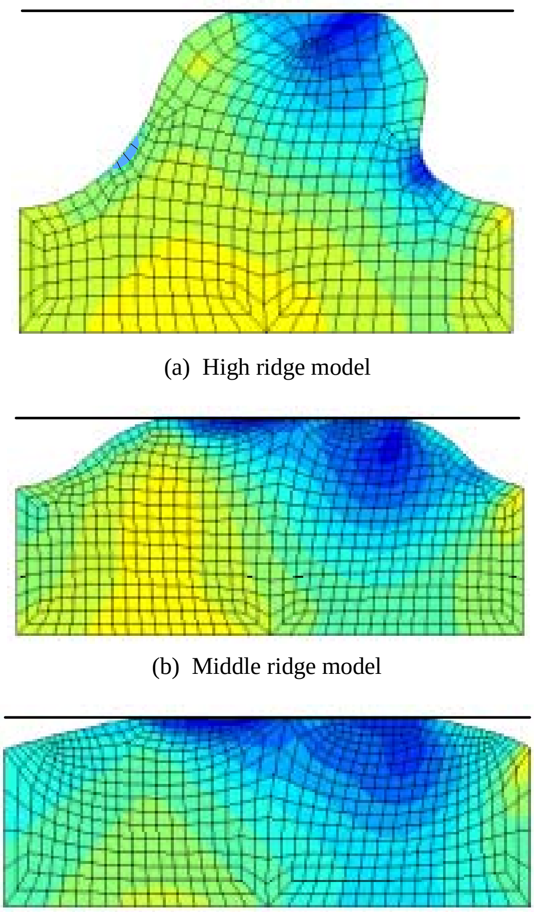

(a) High ridge model

(b) Middle ridge model

(c) Low ridge model

Fig. 3 Distribution of strain inside the ridge

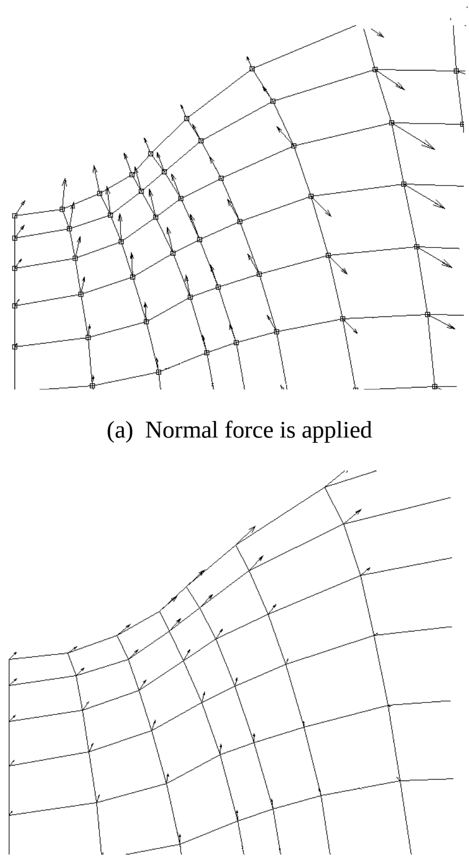

(a) Normal force is applied

(b) Normal and tangential forces are applied

Fig. 4 Principal strain distribution near the edge of the ridge

strains at two points corresponded to the FA I receptors is almost zero. Then the tangential deformation of the ridge cannot be identified by the subtracted value. On the other hand, the strain inside the ridge is asymmetry with producing strong stress concentration in the model having middle ridge as shown in Fig.3 (b). Therefore, we decided the shape of the ridge to be the middle ridge model.

Second, locations and directions to detect the pair of strain inside the ridge are decided. A FE model of the ridge, which has same geometry as the middle ridge model, is made in detail. We analyzed a relationship between the directions of external force and principal strain inside the ridge. Results are as follows: Only when the normal force is applied, the direction of principal strain at the location correspond to that of FA I receptors is almost vertical as shown in Fig. 4 (a). However, when both the normal and tangential forces are applied, the direction of principal strain at the same location is inclined to about 45 degrees as shown in Fig. 4 (b). Consequently, a relationship between the tangential deformation of the ridge and the subtracted value of strains can be calculated. So, the location and direction are decided as shown in Fig. 5.

Third, a radius of curvature for artificial finger skin is decided. If the radius is too large, normal contact force does not distributed and the partial slippage of the ridge at

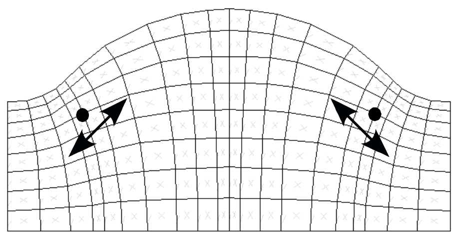

Fig. 5 Points and directions for subtracting the strains

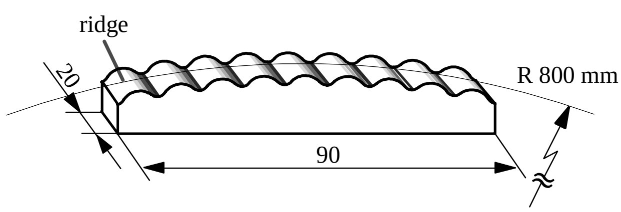

Fig. 6 Top view of designed artificial finger skin

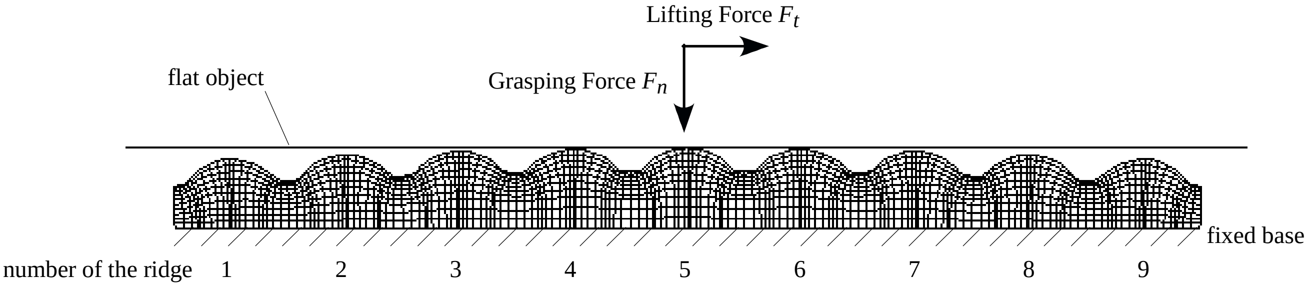

Fig. 7 Two dimensional FE model of designed artificial finger skin

Table 1 Parameters of each analysis

case	friction coefficient static	friction coefficient kinetic	maximum value of grasping force	time step size	total time step number
basic case	1.05	1.00	4 N	1.0×10^{-6} s	550
case 1	1.58	1.50	4 N	1.0×10^{-6} s	550
case 2	0.63	0.60	4 N	1.0×10^{-6} s	650
case 3	0.32	0.30	4 N	1.0×10^{-6} s	650
case 4	1.05	1.00	2 N	1.0×10^{-6} s	450
case 5	1.05	1.00	4 N	2.0×10^{-6} s	1100

the edge of the contact area does not surely occur. If the radius is too small, contact area is too small and ridges at the edge of the artificial finger skin does not in contact, even when a large normal force is applied. The radius is decided to be 800 mm by considering the above-mentioned condition. The number of ridges is nine so as to detect the partial incipient slippage conspicuously, even when the contact area changes due to the change in value and direction of the normal contact force.

It is expected by FE analysis that all the ridges are in contact with a flat object when the normal force of 4 N is applied, so the assumed limit of the weight of the object is about 4 N when the static friction coefficient is 1.0. Artificial finger skin is designed from above-mentioned decisions as shown in Fig. 6.

3. Analysis of performance of artificial finger skin

3.1 FE model

A FE model of the designed entire artificial finger skin is made for analyzing the dynamic contact condition between the finger and a flat object. A purpose of the analysis is to confirm feasibility of the method that the entire slippage of the ridge at the edge of contact area can be detected by use of the velocity and acceleration of strains inside the ridge, even when the applied force, the friction coefficient and the speed of applied of force are changed. The FE model of the designed artificial finger skin is shown in Fig. 7. Displacement at the bottom edge of the artificial finger skin is fixed. The flat object is defined as a rigid body. Then, an external force is applied by changing the position of the flat object. The external force

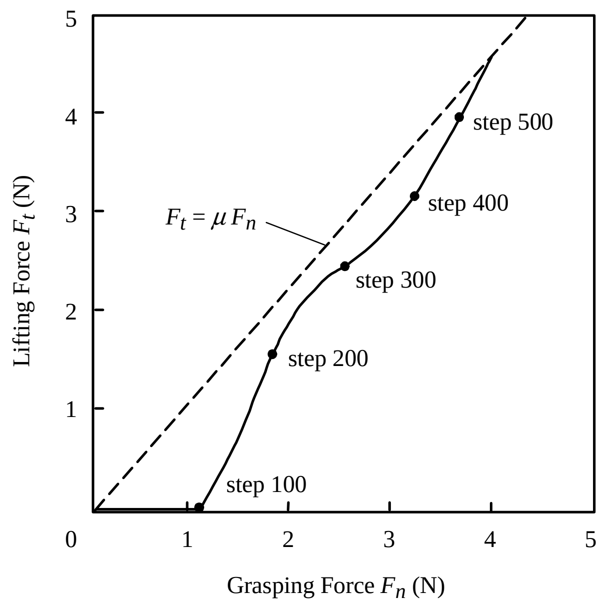

Fig. 8 History of external force

consists of grasping force F_n and lifting force F_t. The direction of the grasping force is vertical to the base of artificial finger skin. The direction of the lifting force is horizontal to the base. The ridges are numbered from one to nine for identifying each other. Material properties are as follows: Young's module of artificial finger skin is 4.96 MPa. Poison's ratio is 0.49. Mass density is 1230 kg/m^3. Mechanical material type of finger is isotropy. These material properties are similar to those of silicone rubber.

3.2 Condition of calculation

The external force is applied as shown in Fig. 8. Only the grasping force is applied at first for avoiding entire slippage when the lifting force is started to be applied. Then, the grasping and lifting force are increased. The partial incipient slippage easily occurs from time step 200 to 300, because divided value F_t / F_n is close to static friction coefficient. Then the partial incipient slippage does not easily occur from the step 300 because the divided value F_t / F_n is smaller than the static friction coefficient. And then, the partial incipient slippage easily occurs again from time step 450 toward the entire slippage. All the time is divided into 550 steps. Time of one step is 1.0×10^{-6} s. The natural frequency and natural cycle of the ridge is 7680 Hz and about 1.3×10^{-4} s, respectively. Now, the time step size is selected to be small enough compared with the natural cycle of the ridge so as to analyze the dynamic deformation of ridges due to the partial incipient slippage. Kinetic friction coefficient is 1.0. Static friction coefficient is 1.05.

Above-mentioned condition is called a “basic case”. Analyses for some other cases are also conducted when several parameters are changed as shown in Table 1. The changed parameters are friction coefficient, maximum value of grasping force, time step size and total time step number throughout the analysis.

3.3 Results of analysis

First, an analysis for the basic case is conducted. Histories of number for sticking nodes in the third and fifth ridge are shown in Fig. 9.

As shown in Fig. 9 (a), the number of sticking nodes of the fifth ridge is zero at first. It gradually increases and reaches seven at the time step 263. The gradual increase of stick area is due to the increase of grasping force. As the fifth ridge is located at the center of the finger, the lifting force is largest compared with other ridges. So the stick area increases and reaches a large number, seven. In the time steps 120, 170 and 230, the number suddenly decreases and increases again. It is due to the following reason. At these time steps, the grasping force is not large and the contact area throughout the finger is still small. So a part of the contact area easily slips. Then, a partial incipient slippage in the fifth ridge occurs. At the time step 450, the number of sticking nodes is slightly decreased. It is due to the entire slippage of the third ridge as described as follows.

Figure 9 (b) shows the change in the number of sticking nodes in the third ridge. The number of the sticking nodes gradually increases from zero to seven and suddenly decreases in the time step 450. The gradual increase is due to the increase of the grasping force. The sudden decrease is due to the entire slippage of this ridge. As the ratio between F_t / F_n is approaching towards the static friction coefficient at time step 450 as shown in Fig. 8, the ridges at the edge of entire finger easily slip as expected in chapter 2. Now, the predicted phenomena are seen in the results of FE dynamic contact analysis.

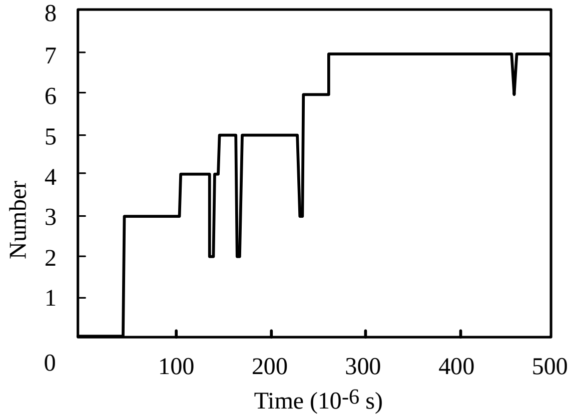

(a) Fifth ridge

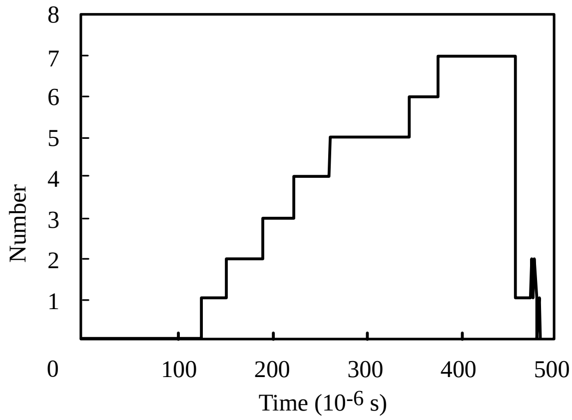

(b) Third ridge

Fig. 9 Number of nodes which sticks

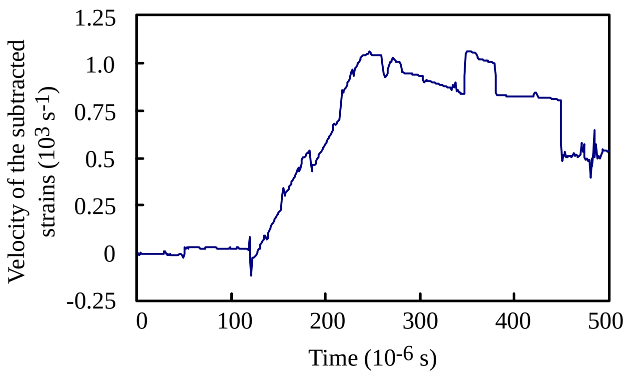

Fig. 10 Velocity of the subtracted strains inside third ridge

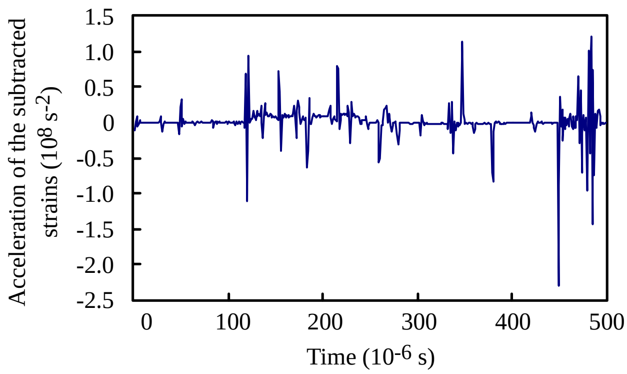

Fig. 11 Acceleration of the subtracted strains inside third ridge

First and second time derivatives of the subtracted strains inside the third ridge, which we call a velocity and an acceleration of subtracted strains, are shown in Fig. 10 and Fig. 11, respectively. The velocity of the third ridge increases gradually from time step 120 to 380. Then, it decreases when the partial incipient slippage occurs at time step 450, because the tangential deformation is released when local entire slippage occurs at the third ridge. Stepwise changes in the velocity are seen at time step 160, 190, 340 and 380. This is due to the change in contact condition of neighboring ridges. The acceleration of the third ridge responds with large amplitude at time step 450 as shown in Fig 11, because the velocity decreases as shown in Fig. 10. An absolute value of the amplitude of the acceleration is larger than 2.0×10^8 s^{-2}. On the other hand, the large response of acceleration is not seen in the fifth ridge at the same time, because the entire slippage of the fifth ridge doesn't occur even when the slippage of the third ridge occurs.

Analyses for other case are also conducted. Phenomena agree well with those of the basic case, even when some parameters are changed. The partial incipient slippage occurs when the contact condition of ridges at the edge of contact area is changed from “stick” to “slip”. Stepwise decreases of the velocity of subtracted strains are surely seen at the ridge at the edge of contact area when the entire slippage of the ridge occurs. Then, the absolute values of the amplitude of the acceleration are always larger than 2.0×10^8 s^{-2} when the entire slippage of a certain ridge occurs.

Consequently, the velocity of subtracted strains inside the ridge largely decreases when the contact condition changes from “stick” to “slip” because the entire slippage of the ridge at the edge of the contact area occurs. The absolute value of the amplitude of acceleration is always larger than 2.0×10^8 s^{-2} at the ridge which slips. Therefore, the partial incipient slippage can be detected by the change in velocity and the absolute value of the acceleration of ridges at the edge of the entire contact area as expected in chapter 2. The pair of strains underneath the ridges can be practically measured by placing strain gages of PVDF films at these points. Now, the grasping force and listing force can be controlled as follows: First, the contact condition of the ridge at the edge of the contact area is monitored. Then, if it slips, normal grasping force is increased to prevent from entire slippage. Otherwise, tangential lifting force is increased. By continuing this procedure, objects whose weight and friction coefficient are unknown can be grasped and lifted.

The method is considered to be the same as that of human do because human seems to detect the partial incipient slippage wherever the contact surface exists. Therefore, the proposed method for detecting the partial incipient slippage should be extended to develop a two-dimensional finger pad. The designed artificial finger skin will be made for conducting an experiment for controlling a grasping force in future studies.

4. Conclusions

An elastic finger skin is proposed for grasping an object whose weight and friction coefficient are unknown. It has a unique geometry imitating a configuration of ridges and FA I receptors of finger of human. First, precise geometry of the artificial finger skin is designed using FE analysis. Then, it is confirmed by FE analysis that the partial incipient slippage of the ridges at edge of the contact area is detected by change in velocity and acceleration of the subtracted value of strains inside the ridges where strain sensors are placed.

5. Acknowledgements

This study is partly supported by a Grant-in-Aid for Scientific Research (#12450168) from Japan Society for the Promotion of Science, The Ministry of Education, Culture, Sprots, Science, and Technology.

6. Reference

[1] R. S. Johansson and G. Westling, “Roles of Glabrous Skin Receptors and Sensorimotor Memory in Automatic Control of Precision Grip When Lifting Rougher of More Slippery Objects”, *Exp. Brain Res.*, Vol. 56, pp. 550-564,1984.

[2] R. S. Johansson and G. Westling, “Signals in Tactile Afferents from the Fingers Eliciting Adaptive Motor Responses During the Precision Grip”, *Exp. Brain Res.*, Vol. 66, pp. 141-154, 1988.

[3] R. D. Howe and M. R. Cutkosky, “Sensing Skin Acceleration for Slip and Texture Perception”, *Proc. IEEE Int. Conf. Robotics and Automation*, Vol. 1, pp. 145-150, 1989.

[4] M. R. Tremblay and M. R. Cutkosky, “Estimation of Friction Using Incipient Slip Sensing During a Manipulation Task”, *Proc. IEEE Int. Conf. Robotics and Automation*, Vol. 1, pp. 429-434, 1993.

[5] G. Canepa, R. Petrigliano, M. Campanella and D. De Rossi, “Detection of Incipient Object Slippage by Skin-Like Sensing and Neural Network Processing”, *IEEE. Trans. on Systems, Man, and Cybernetics -- part B:Cybernetics*, Vol. 28, No. 3, pp. 348-356, 1998.

[6] T. Maeno, K. Kobayashi and N. Yamazaki, “Sensing Mechanism of the Partial Incipient Slip at the Surface of Cylindrical Fingers During the Precision Grip”, *Proc. ASME Summer Bioengineering Conf.*, pp. 117-118, 1997.

[7] T. Maeno, T. Kawai and K. Kobayashi, “Analysis and Design of a Tactile Sensor Detecting Strain Distribution inside ad Elastic Finger”, *Proc. IEEE/RSJ Int. Conf. Intelligent Robots and Systems*, pp. 1658-1663, 1998.

[8] T. Maeno, S. Hiromitsu and T. Kawai, “Control of Grasping Force by Detecting Stick/Slip Distribution at the Curved Surface of an Elastic Finger”, *Proc. IEEE Int. Conf. Robotics and Automation*, pp. 3896-3901, 1999.

[9] Y. Yamada, Y. Morita and Y. Umetani, “Slip phase isolating : impulsive signal generating vibrotactile sensor and its application to real-time object re-grip control”, Robotica, Vol. 18, No. 1, pp.43-49, 2000.